Letter

New energy for the 133-keV resonance in the ^{23}Na(p, γ) ^{24}Mg reaction and its impact on nucleosynthesis in globular clusters

C. Marshall ⬤,[*] K. Setoodehnia ⬤,[†] F. Portillo ⬤, J. H. Kelley ⬤, and R. Longland ⬤

Department of Physics, North Carolina State University, Raleigh, North Carolina 27695, USA
and Triangle Universities Nuclear Laboratory, Durham, North Carolina 27708, USA

Globular cluster stars exhibit star-to-star anticorrelations between oxygen and sodium in their atmospheres. An improved description of the sodium-destroying ^{23}Na $+$ p reaction rates is essential to understanding these observations. We present an energy analysis of ^{24}Mg states based on a new measurement of the ^{23}Na(^{3}He, d) ^{24}Mg reaction. A key resonance in ^{23}Na(p, γ) ^{24}Mg is found to be at $E_r^{\text{c.m.}} = 133(3)$ keV, 5 keV lower than previously adopted. This finding has a dramatic effect on the ^{23}Na(p, γ) ^{24}Mg reaction rate, increasing it by a factor of 2 for the recommended rate. The nucleosynthesis impact of this change is investigated.

DOI: 10.1103/PhysRevC.104.L032801

Globular clusters consisting of hundreds of thousands of gravitationally-bound stars have been found to be some of the oldest structures in the galaxy (see, for example, Ref. [1]). They are thought to have formed from homogeneous clouds of gas and have evolved without external influence [2]. Consequently, globular clusters can be used as simple, isolated stellar laboratories to better understand the evolution of the elements in stars.

Star-to-star variations in observational signatures, however, have long been apparent in globular clusters, pointing to a more complex evolution. In particular, the advent of high-resolution spectroscopic measurements of the atmospheres of stars within globular clusters have revealed correlations between sodium and aluminum, as well as sodium-oxygen and magnesium-aluminium anticorrelations (see Refs. [3] and [4] for a review). The sources for these anticorrelations are still unknown [5]. However, they must arise from a previous generation of "polluter" stars, as the observed elements cannot be produced *in situ*. Identifying the polluter stars has proved challenging, but possible candidates are massive rotating or nonrotating Asymptotic Giant Branch (AGB) stars [6–11], rotating massive stars [12,13], and massive binaries [14]. New physical models of dredge-up episodes in red giant branch stars may also be needed to explain the Na-O anticorrelation [15].

The sodium-destroying ^{23}Na $+$ p reactions, ^{23}Na(p, γ) ^{24}Mg and ^{23}Na(p, α) ^{20}Ne, play a critical role in explaining the Na-O anticorrelation in globular clusters [16]. They represent a key branching point in hydrogen burning beyond the CNO cycle, determining both how quickly sodium can be destroyed in the stellar environment, and how much of that material is cycled back into the Ne-Na cycle vs transferred into the Mg-Al mass range. Currently, the ^{23}Na $+$ p reaction rates are not well constrained between $T = 40$ MK and $T = 100$ MK where the stars are burning their fuel [16,17]. Thus, the outputs of stellar models aimed at understanding the Na-O anticorrelation are not reliable at present.

The strengths of important resonances in the ^{23}Na(p, γ) ^{24}Mg and ^{23}Na(p, α) ^{20}Ne reactions have long been under investigation. The proton scattering results of Ref. [18] and recoil-coincidence measurements of Ref. [19] identified the energies of resonances most strongly impacting the reaction rates. Those resonances were first measured directly for the ^{23}Na(p, γ) ^{24}Mg and ^{23}Na(p, α) ^{20}Ne reactions in Refs. [20] and [21], respectively. While an important resonance in ^{23}Na(p, α) ^{20}Ne at $E_r^{\text{c.m.}} = 178$ keV was measured, the strength of the key resonance potentially impacting both reaction rates at $E_r^{\text{c.m.}} = 138$ keV could not be determined. A ^{23}Na(^{3}He, d) ^{24}Mg proton transfer measurement by Hale *et al.* [22] was used to estimate strengths of resonances in the ^{23}Na $+$ p reactions. However, the authors were unable to unambiguously determine the spin-parity of the 138-keV resonance, and the reaction rate retained large uncertainties. Since then, direct measurements of the 138-keV resonance in ^{23}Na(p, γ) ^{24}Mg were attempted, yielding resonance strength upper limits of $\omega\gamma \leqslant 1.5 \times 10^{-7}$ eV [23] and $\omega\gamma \leqslant 5.17 \times 10^{-9}$ eV [16]. The latter measurement found evidence for the resonance, but chose to report an upper limit of its strength because their result was not significant on the 3σ level. They suggested a resonance strength of $\omega\gamma = 2.15 \pm 1.29 \times 10^{-9}$ eV under the assumption of a positive detection. Reference [16] also ruled out the 138-keV resonance as a significant contributor to the ^{23}Na(p, α) ^{20}Ne reaction rate. Recently, the resonance was reported with a statistical significance above 2σ with $\omega\gamma = 1.46^{+0.58}_{-0.53} \times 10^{-9}$ eV [17], in agreement with Ref. [16], but with significantly reduced uncertainties.
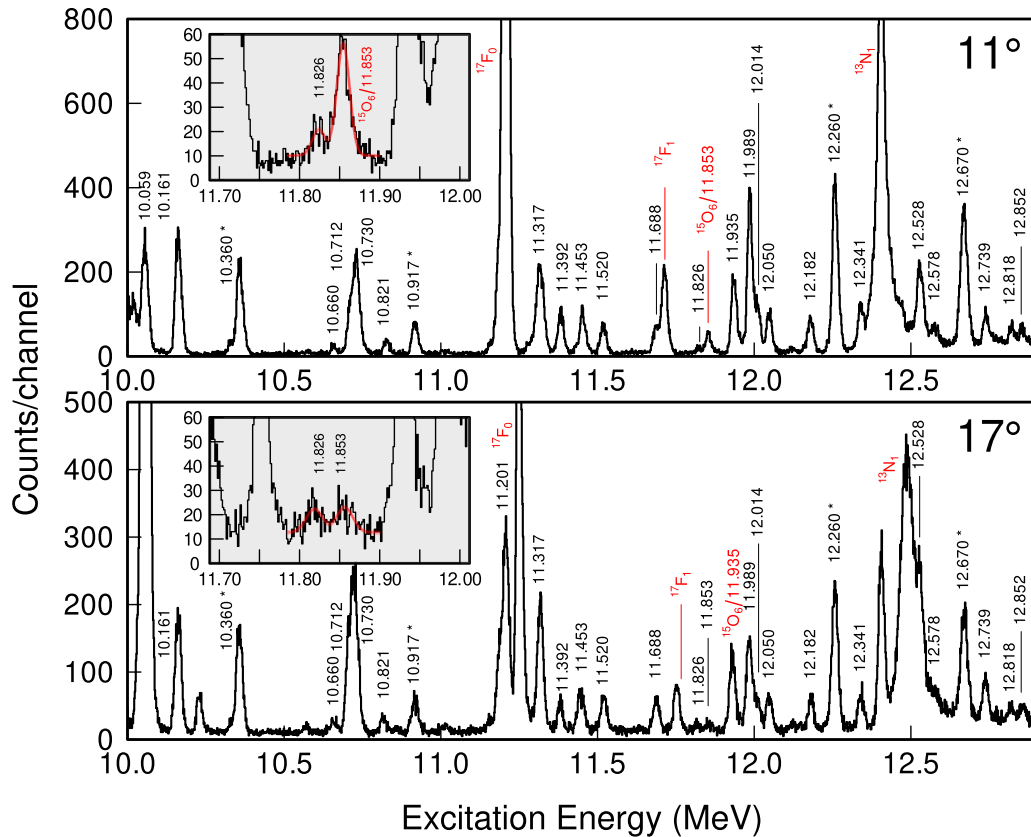
FIG. 1. Part of the calibrated deuteron focal plane spectra from the ^{23}Na(^{3}He, d)^{24}Mg reaction collected at laboratory angles of 11° and 17°. The binned counts are plotted as a function of excitation energy in ^{24}Mg with the corresponding states labelled with their adopted energies in MeV. States with asterisks were used as calibration points (7 in total, some fall outside the plotted range). Highlighted states (red) correspond to background lines from target contaminants and are labeled with their corresponding excited state. For example, ^{17}F$_1$ labels the 1st excited state in ^{17}F, which is populated by ^{16}O(^{3}He, d)^{17}F on oxygen contamination in the target. The insets provide the region around the important $E_x = 11\,826$ keV state with fits to the peaks depicted in red.

Despite these successes, significant errors in the rate could exist because of inaccurate resonance energies. Charged particle reaction rates dominated by narrow resonances have an exponential dependence on resonance energies. Weak resonances measured with low-counting statistics usually do not provide reliable resonance energy estimates [16,17,20,23]. As a result, the most recent reaction rate calculations were performed using energies suggested from the proton transfer reaction reported in Ref. [22].

Here, we report on a new proton transfer measurement to determine the energies of states in ^{24}Mg. We find that the energy of the $E_x = 11\,826$ keV state, corresponding to the important $E_r^{\text{c.m.}} = 133$ keV resonance, is 5 keV lower than previously recommended, and this result impacts the ^{23}Na(p, γ)^{24}Mg reaction rate strongly. A subsequent paper will report on the full collection of states observed in our measurement [24].

In addition to the excitation energies inferred in this work, above 11 MeV there are a number of updates to other level energies reported in the ENSDF evaluation [25]: (i) the latter was incomplete and did not include results from Refs. [20] and [22]; (ii) there have been additional measurements in the intervening 13 years; (iii) the mass evaluation of Ref. [26] affects the excitation energies deduced from the ^{20}Ne(α, γ)^{24}Mg

and ^{23}Na(p, γ)^{24}Mg resonance energies; and (iv) upon close inspection, it is apparent that Ref [25] used γ-ray energies from Ref. [27], which were not reported, but rather inferred from level energy differences, thus introducing artificially small uncertainties when a least-squares fit was performed to obtain the ENSDF values. As such, excitation energies were carefully compiled separately for this paper using reported energies in Refs. [18–20,27–32]. The full compilation is available in Ref. [33] and will be presented in an accompanying paper [24]. Only the astrophysically important state at $E_x = 11\,826$ keV is addressed below. Note that the reevaluated energy uncertainties are generally *larger* than those presented in Ref. [25] due to the error discussed above.

The proton transfer experiment was performed at the Triangle Universities Nuclear Laboratory (TUNL) using the Enge split-pole spectrograph. The instrument is located at the end of the high-resolution beamline at the TUNL Tandem accelerator laboratory, where two 90-degree dipole analyzing magnets deliver beams of precisely controlled energies to the target. In the measured spectra, (see Fig. 1), background contaminants arise from reactions with kinematics different from that of the ^{23}Na(^{3}He, d)^{24}Mg reaction of interest. A ^{3}He^{++} beam energy of 21 MeV was chosen to minimize the presence of those contaminants in spectral areas where the astrophysically-

important states appear. The beam was then tuned through a 1-mm collimator at the target position to ensure good optical focusing of reaction products onto the focal plane. The NaBr targets were placed on a target ladder along with a natural carbon backing foil for background identification. The beam current was monitored with an electron-suppressed beam stop downstream from the targets. A silicon telescope was placed at 45° to monitor target degradation, and beam fluctuations, and to normalize the data.

Targets were produced under vacuum by thermally evaporating NaBr powder onto $22\,\mu g/cm^2$-thick natural carbon backing foils. The NaBr thickness, as measured with a thickness monitor during evaporation, was approximately $70\,\mu g/cm^2$. The exact sodium concentration was not required for the experiment since the measurement was performed relative to the elastic scattering cross section. Furthermore, the energy calibration using well-known states in ^{24}Mg did not require exact knowledge of energy loss in the targets. The evaporation was performed within a few hours of the start of the experiment to minimize target oxidation.

Reaction products from the target entered the Enge split-pole spectrograph through a 1 msr aperture and were momentum-analyzed with a magnetic field strength of $B = 1.13 - 1.14$ T so as to focus deuterons from the astrophysically-important states on the focal plane detector. Deuteron peaks arising from 54 ^{24}Mg states at $E_x = 7364 - 12\,965$ keV were observed. More details can be found in Ref. [33]. Deuterons were clearly identified with a ΔE vs E cut. Example focal plane spectra for deuterons at $\theta_{lab} = 11°$ and $17°$ are shown in Fig. 1. Deuteron spectra were collected at angles between $3° - 21°$ in steps of $2°$ with an additional measurement at $26°$.

These spectra were internally calibrated using precisely known states in ^{24}Mg, some of which are highlighted with asterisks in Fig. 1. To ensure a robust energy calibration, a wide range of excitation energies were considered, covering the entire focal plane: $E_x = 8654.53(15)$, $8864.29(9)$, $9457.81(4)$, $10360.51(13)$, $10\,916.96(17)$, $12\,257.69(21)$, and $12\,669.9(2)$ keV. For calibration energies above 11 MeV, we adopted the value obtained from the procedure described above. The peak centroids were obtained by fitting Gaussian line-shapes and linear backgrounds, which were found to reproduce the data well. The spectrum was then fit with a 3rd-order polynomial using the Bayesian method outlined in Ref. [34]. The Bayesian Markov chain Monte Carlo calibration method utilizes a relativistic kinematics calculation to predict the magnetic rigidity of deuterons corresponding to each excited state in ^{24}Mg. Rather than undergoing an iterative procedure to convert peak centroid channel numbers to uncertainties in energy, the channel number and energy uncertainties are explicitly included in the two-dimensional Bayesian calibration model. For this particular problem, the Ensemble Sampler [35] from the python package, `emcee` [36], was found to be efficient. Excitation energies extracted individually at each angle were found to be consistent with each other. The averaging method from Ref. [37] was used to combine these results, accounting for systematic effects. More details on the calibration can be found in Ref. [33]. Over the entire focal plane, most states are in good agreement with the literature

TABLE I. Excitation energies (in keV) for the state corresponding to the $E_r^{c.m.} = 133$ keV resonance. The result from Ref. [22] was not used in the average, adopted value (see text).

Source	Energy (keV)
This paper	11 823 (3)
Moss *et al.* 1976[a]	11 828 (3)
Vermeer *et al.* 1988[b]	11 827 (4)
Hale *et al.* 2004[c]	11 831.7 (18)
Adopted	11 826 (3)

[a]Reference [18].
[b]Reference [19].
[c]Reference [22].

energies with an average deviation of 1.3-σ, as indicated in Fig. 1. For the state in question, we determined an excitation energy of $E_x = 11\,823(3)$ keV.

A weighted average of the compiled energies from the measurements presented here was then performed to determine adopted energies for the reaction rate calculations. Table I demonstrates this procedure for the state corresponding to the $E_r^{c.m.} = 133$ keV resonance. The results from Ref. [22] were not included for the reasons explained in detail below. We applied the convention that for 3 or fewer measurements, the smallest reported uncertainty is adopted for the final value.

We recommend an energy of $E_x = 11\,826(3)$ keV [$E_r^{c.m.} = 133(3)$ keV] for the astrophysically-important state. This value agrees within uncertainties with that reported by Ref. [25] at $11\,827(4)$ keV, but disagrees with the energy recommended by Hale *et al.* at $11\,830.7(15)$ keV [22]. The difference between the two spectrograph measurements (the one presented here and that of Ref. [22]) is understood and its origin is twofold: (i) A relatively narrow region of energies was used to calibrate the detector in Ref. [22]; and (ii) one calibration peak was erroneously assumed to be correspond to the $E_x = 11\,330$ keV state, rather than the one at $E_x = 11\,317$ keV. The combined effect of these led to a strongly skewed quadratic energy calibration in the astrophysically-important region. This hypothesis is confirmed by testing the calibration presented in Ref. [22] with the peak centroids from the present paper. In the present paper, the detector is calibrated over a wide energy range, ensuring a robust calibration that matches the quadratic response of the spectrograph [38]. To avoid any confusion, the state used by Ref. [22] was not included in the calibration presented here. This effect influences several of the states measured by Ref. [22], although most of these have well-known energies from other measurements.

Our new energy for the $E_r^{c.m.} = 133$ keV resonance was then used to calculate an updated reaction rate. The rate is calculated using the `RatesMC` Monte Carlo reaction rate code first introduced in Ref. [39] and subsequently updated to enable new features in Refs. [40–42]. The general procedure is to assign a statistically-motivated probability density distribution to every uncertain reaction rate input parameter. Those probability distributions are then sampled to calculate the reaction rate many (10 000) times. The end result is a temperature-dependent reaction rate probability distribution
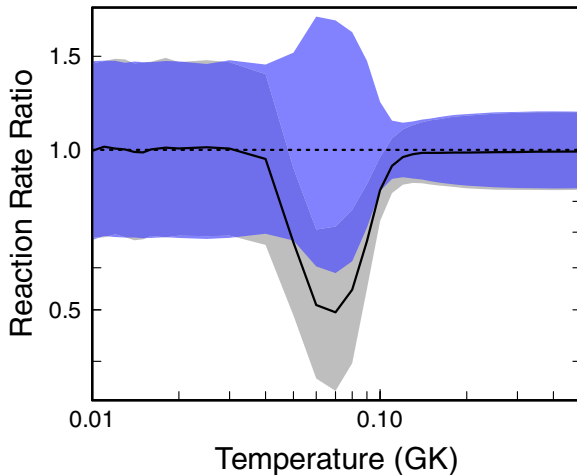
FIG. 2. Reaction rate ratio for the ^{23}Na(p, γ) ^{24}Mg reaction: shown as a blue shaded region are the present temperature-dependent 1-sigma reaction rate uncertainties ("high" and "low" rates) normalized to the recommended rate. The solid-black line represents the recommended rate from Ref. [17], with grey shaded region corresponding to the associated 1-sigma uncertainty.

that can be summarised by a recommended rate and an uncertainty. The resonance parameters are adopted from Iliadis *et al.* [43] as a baseline with updates from Cesaratto *et al.* [16] and Boeltzig *et al.* [17]. Resonance energies are calculated using the 2016 mass evaluation of Ref. [26] with a ^{23}Na(p, γ) ^{24}Mg Q-value of $Q_{(p,\gamma)} = 11\,692.690(10)$ keV. Our modified energy for the 133-keV resonance is then applied accordingly.

The result for the ^{23}Na(p, γ) ^{24}Mg reaction is shown in Fig. 2 in comparison to that calculated using the most recent resonance parameters from Boeltzig *et al.* [17]. Both are displayed as a ratio to the present recommended rate to highlight differences between the two rates. The blue shaded region depicts the present temperature-dependent uncertainty, while the grey shaded area and black solid line display the results from Ref. [17]. The solid line is the recommended rate from Ref. [17] and the shaded region covers their reported high and low rate corresponding to 68% confidence limits. It is clear from the figure that the new resonance energy reported here has a dramatic effect on the recommended reaction rate, increasing it by a factor of 2 over the previous one at the astrophysically-important temperatures. This significant difference arises from the energy of the $E_r^{\text{c.m.}} = 133$ keV resonance. Lowering the energy by 5 keV compared to the value used by Ref. [17] moves the resonance closer to the center of the Gamow window. Assuming that the measured resonance strength remains constant, the reaction rate increases

exponentially with a lower resonance energy. Although not investigated here, this lowering of the resonance energy may also have profound impacts on the interpretation of the results from Refs. [16] and [17]. Those results must assume that the resonance reactions occur close to the center of the thick target being used. However, if the resonance energy is lower than expected, the physical location of the resonant reactions may be located in a region of the target with less ^{23}Na concentration. Thus, the resonance strength may be even more drastically affected by the results presented here.

The reaction rate was used in a nucleosynthesis calculation in order to investigate its impact. A single-zone nucleosynthesis calculation was performed with a constant temperature and density of $T = 75$ MK and $\rho = 10\,\text{g/cm}^3$ and an initial composition taken from Ref. [44]. The initial mass fraction of hydrogen was $X(H) = 0.75$ and the nucleosynthesis calculation was run until this was reduced to $X(H)_{\text{final}} = 0.075$. The standard set of reaction rates from the STARLIB library [45] were adopted, while changing only the ^{23}Na(p, γ) ^{24}Mg and reverse ^{24}Mg(γ, p) ^{23}Na reactions (the latter will not affect the outcome at these low temperatures).

These calculations lead to a median drop of 50% in the final predicted ^{23}Na abundance when using the present rates, and a corresponding increase by a factor of 2.5 in the final ^{24}Mg abundance. The uncertainty in these nucleosynthesis yields is also larger, given the larger energy uncertainty for the key $E_r^{\text{c.m.}} = 133$ keV resonance. Stellar models typically have great difficulty producing the required sodium abundance in globular clusters [12], so any reduction has the potential to significantly impact our understanding of their evolution. Clearly, the energy of the $E_r^{\text{c.m.}} = 133$ keV resonance has an influential impact on nucleosynthesis during hydrogen burning at the temperatures considered here. Further γ-ray studies to precisely determine the energy of resonances between the proton threshold and 300 keV in the ^{23}Na +p reactions are encouraged so that yields from stellar models can be reliably used to understand globular cluster anomalies.

[1] D. A. VandenBerg, M. Bolte, and P. B. Stetson, Annu. Rev. Astron. Astrophys. **34**, 461 (1996).

[2] D. A. Forbes, N. Bastian, M. Gieles, R. A. Crain, J. M. D. Kruijssen, S. S. Larsen, S. Ploeckinger, O. Agertz, M. Trenti, A. M. N. Ferguson *et al.*, Proc. R. Soc. A **474**, 20170616 (2018).

[3] R. Gratton, C. Sneden, and E. Carretta, Annu. Rev. Astron. Astrophys. **42**, 385 (2004).

[4] S. Cassisi and M. Salaris, Astron. Astrophys. Rev. **28**, 5 (2020).

[5] A. Slemer, P. Marigo, D. Piatti, M. Aliotta, D. Bemmerer, A. Best, A. Boeltzig, A. Bressan, C. Broggini, C. G. Bruno, A.

Caciolli, F. Cavanna, G. F. Ciani, P. Corvisiero, T. Davinson, R. Depalo, A. Di Leva, Z. Elekes, F. Ferraro, A. Formicola *et al.*, Mon. Notices Royal Astron. Soc. **465**, 4817 (2017).

[6] P. Ventura, F. D'Antona, I. Mazzitelli, and R. Gratton, Astrophys. J. **550**, L65 (2001).

[7] F. D'Antona, V. Caloi, J. Montalbán, P. Ventura, and R. Gratton, Astron. Astrophys. **395**, 69 (2002).

[8] P. A. Denissenkov and F. Herwig, Astrophys. J. **590**, L99 (2003).

[9] T. Decressin and C. Charbonnel, in *From Lithium to Uranium: Elemental Tracers of Early Cosmic Evolution*, edited by V. Hill, P. Francois, and F. Primas, IAU Symposium, Vol. 228 (Cambridge University Press, 2005), pp. 395–396.

[10] P. Ventura, M. Di Criscienzo, R. Carini, and F. D'Antona, Mon. Notices Royal Astron. Soc. **431**, 3642 (2013).

[11] C. L. Doherty, P. Gil-Pons, H. H. B. Lau, J. C. Lattanzio, and L. Siess, Mon. Notices Royal Astron. Soc. **437**, 195 (2014).

[12] N. Prantzos and C. Charbonnel, Astron. Astrophys. **458**, 135 (2006).

[13] T. Decressin, G. Meynet, C. Charbonnel, N. Prantzos, and S. Ekström, Astron. Astrophys. **464**, 1029 (2007).

[14] S. E. de Mink, O. R. Pols, N. Langer, and R. G. Izzard, Astron. Astrophys. **507**, L1 (2009).

[15] J.-W. Lee, Mon. Notices Royal Astron. Soc. **405**, L36 (2010).

[16] J. M. Cesaratto, A. E. Champagne, M. Q. Buckner, T. B. Clegg, S. Daigle, C. Howard, C. Iliadis, R. Longland, J. R. Newton, and B. M. Oginni, Phys. Rev. C **88**, 065806 (2013).

[17] A. Boeltzig, A. Best, F. R. Pantaleo, G. Imbriani, M. Junker, M. Aliotta, J. Balibrea-Correa, D. Bemmerer, C. Broggini, C. G. Bruno *et al.*, and Phys. Lett. B **795**, 122 (2019).

[18] C. E. Moss, Nucl. Phys. A **269**, 429 (1976).

[19] W. J. Vermeer, D. M. Pringle, and I. F. Wright, Nucl. Phys. A **485**, 380 (1988).

[20] J. Goerres, M. Wiescher, and C. Rolfs, Astrophys. J. **343**, 365 (1989).

[21] J. Zyskind, M. Rios, and C. Rolfs, Astrophys. J. **243**, L53 (1981).

[22] S. E. Hale, A. E. Champagne, C. Iliadis, V. Y. Hansper, D. C. Powell, and J. C. Blackmon, Phys. Rev. C **70**, 045802 (2004).

[23] C. Rowland, C. Iliadis, A. E. Champagne, C. Fox, J. José, and R. Runkle, Astrophys. J. **615**, L37 (2004).

[24] C. Marshall, K. Setoodehnia, J. H. Kelley, F. Portillo, and R. Longland (unpublished).

[25] R. B. Firestone, Nucl. Data Sheets **108**, 1 (2007).

[26] W. J. Huang, G. Audi, M. Wang, F. G. Kondev, S. Naimi, and X. Xu, Chin. Phys. C **41**, 030002 (2017).

[27] P. Schmalbrock, H. W. Becker, L. Buchmann, J. Görres, K. U. Kettner, W. E. Kieser, H. Kräwinkel, C. Rolfs, H. P. Trautvetter, J. W. Hammer, and R. E. Azuma, Nucl. Phys. A **398**, 279 (1983).

[28] P. J. M. Smulders, Physica **31**, 973 (1965).

[29] B. Zwieglinski, G. M. Crawley, H. Nann, and J. A. Nolen, Phys. Rev. C **17**, 872 (1978).

[30] P. M. Endt, Nucl. Phys. A **521**, 1 (1990).

[31] P. M. Endt, C. Alderliesten, F. Zijderhand, A. A. Wolters, and A. G. M. Van Hees, Nucl. Phys. A **510**, 209 (1990).

[32] L. K. Fifield, M. J. Hurst, T. J. M. Symons, F. Watt, C. H. Zimmerman, and K. W. Allen, Nucl. Phys. A **309**, 77 (1978).

[33] C. Marshall, Investigating globular cluster elemental abundance anomalies using (^{3}He, d) proton transfer reactions, arXiv:2103.08821.

[34] C. Marshall, K. Setoodehnia, K. Kowal, F. Portillo, A. E. Champagne, S. Hale, A. Dummer, and R. Longland, IEEE Trans. Instrum. Meas. **68**, 533 (2018).

[35] J. Goodman and J. Weare, Comm. App. Math. Comp. Sci. **5**, 65 (2010).

[36] D. Foreman-Mackey, D. W. Hogg, D. Lang, and J. Goodman, Publ. Astron. Soc. Pac. **125**, 306 (2013).

[37] M. Schmelling, Phys. Scr. **51**, 676 (1995).

[38] J. E. Spencer and H. A. Enge, Nucl. Instrum. Methods **49**, 181 (1967).

[39] R. Longland, C. Iliadis, A. E. Champagne, J. R. Newton, C. Ugalde, A. Coc, and R. Fitzgerald, Nucl. Phys. A **841**, 1 (2010).

[40] P. Mohr, R. Longland, and C. Iliadis, Phys. Rev. C **90**, 065806 (2014).

[41] R. Longland, Astron. Astrophys. **604**, A34 (2017).

[42] R. Longland and N. de Séréville, Astron. Astrophys. **642**, A41 (2020).

[43] C. Iliadis, R. Longland, A. E. Champagne, and A. Coc, Nucl. Phys. A **841**, 251 (2010).

[44] C. Iliadis, A. I. Karakas, N. Prantzos, J. C. Lattanzio, and C. L. Doherty, Astrophys. J. **818**, 98 (2016).

[45] A. L. Sallaska, C. Iliadis, A. E. Champange, S. Goriely, S. Starrfield, and F. X. Timmes, Astrophy. J. Suppl. **207**, 18 (2013).